Jozef Kačur; Patrik Mihala; Michal Tóth

Numerical modeling of heat exchange and unsaturated-saturated flow in porous media

In: Karol Mikula (ed.): Proceedings of Equadiff 14, Conference on Differential Equations and Their Applications, Bratislava, July 24-28, 2017. Slovak University of Technology in Bratislava, SPEKTRUM STU Publishing, Bratislava, 2017. pp. 191–200.

Persistent URL: http://dml.cz/dmlcz/703050

Proceedings of EQUADIFF 2017
pp. 191–200

NUMERICAL MODELING OF HEAT EXCHANGE AND UNSATURATED-SATURATED FLOW IN POROUS MEDIA*

JOZEF KAČUR†, PATRIK MIHALA‡, AND MICHAL TÓTH§

Abstract. We discuss the numerical modeling of heat exchange between the infiltrated water and porous media matrix. An unsaturated-saturated flow is considered with boundary conditions reflecting the external driven forces. The developed numerical method is efficient and can be used for solving the inverse problems concerning determination of transmission coefficients for heat energy exchange inside and also on the boundary of porous media. Numerical experiments support our method.

Key words. porous media infiltration, water and heat transport, heat energy exchange, numerical modeling of nonlinear system

AMS subject classifications. 65M08, 65M32, 76S05

1. Introduction. In this contribution we discuss the heat transported by infiltrated water into porous media taking into account the heat exchange between infiltrated water and the porous media matrix assuming the flow is unsaturated. This is motivated by an analysis of hygrothermal insulation properties of building facades. The influence of external weather conditions is included in the considered model. We focus especially on the determination of model parameters in a complex mathematical model. Solution of corresponding inverse problems relies on measurements in laboratory conditions using real 3D samples.

The mathematical model consists of the coupled system of strongly nonlinear PDE of elliptic-parabolic type. The flow of water in unsaturated-saturated porous media is governed by Richard's equation. The heat energy transported by infiltrated water is subject to the convection, molecular diffusion, and dispersion, which are driven by external forces due to water and heat fluxes caused by weather conditions. Mathematical models are well known and presented in many monographs, e.g., [1], with very complex list of quotations. Fundamentals of heat and mass transfer with many applications are discussed in [9]. In our setting the heat energy transmission from water in pores to the porous media matrix is treated analogously to the reversible adsorption of contaminant in unsaturated porous media, see e.g. [8],[2]. Additionally, we take into account the heat conduction of the porous media matrix itself. Thus, soluted contaminant in water is replaced by heat energy. Solving the heat conduction of porous media (without water in pores) is difficult task and is modeled by homogenization method. In our setting we assume very simple heat conduction in matrix, where heat permeability is obtained separately by solving a corresponding inverse problem and using practical measurements. We also determine both transmission coefficient

*This work was supported by the Slovak Research and Development Agency APVV-15-0681 and VEGA 1/0565/16.

†SvF STU and FMFI UK Bratislava, Radlinského 11, 810 05, Slovakia (Jozef.Kacur@fmph.uniba.sk).

‡FMFI UK Bratislava, Department of Mathematics, Mlynská dolina, 842 48, Slovakia (pmihala@gmail.com).

§FMFI UK Bratislava, Department of Mathematics, Mlynská dolina, 842 48, Slovakia (m.toth82@gmail.com).

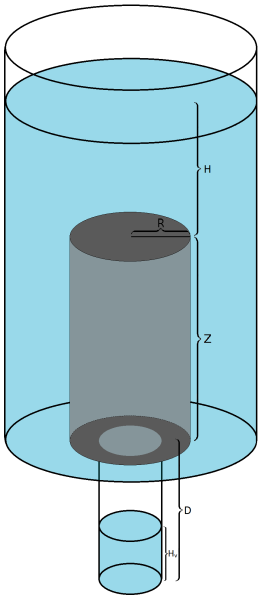

FIG. 1.1. *Sample*

and heat permeability in matrix via the solution of the inverse problem.

Recently, we have discussed in [6] determination of soil parameters in porous media flow model, based on empirical van Genuchten/Mualem capillary/pressure model. There, we have used radially symmetric 3D sample using inflow/outflow measurements. The main reason was that 1D samples (in form of thin tubes) used before suffer from preferential stream lines arising in experiments, especially using centrifugation. We have significantly eliminated this effect by suitable infiltration scenario with cylindrical sample, where infiltration flux from sample mantle is orthogonal to gravitational force. Moreover, the infiltration area is substantially larger then the area of the top of the tube. Thus, we obtained more reliable results in determination of soil parameters. In Fig. 1.1 we sketch the cylinder sample used in experiments.

In this manuscript we present the experiment scenarios to determine transmission, heat conduction and heat boundary transmission coefficients. The heat energy exchange is modeled by temperature gap, water saturation and transmission coefficient. It is almost impossible to measure the temperature gap between the water in pores and in matrix inside the porous media, but we can measure the consequences of heat energy exchange. To determine the heat transmission coefficient and heat conduction coefficient of the matrix we suggest the following experiment scenario. The cylindrical sample is initially uniformly low saturated (almost dry). The temperature of water and matrix is the same, e.g. 20C. Then we let to infiltrate water (through the cylinder mantle) with lower temperature, e.g., 5C. The top and bottom boundary of the cylinder are isolated. We measure the time evolution of temperature in the middle of the top of the cylinder. We note that temperatures of water and matrix in this point (even on whole axis of the cylinder) are the same for long time interval in experiment. The reason is that the infiltrating water has a very sharp front and slowly progresses towards the cylinder axis. Simultaneously the heat is conducted by the matrix and due to the heat exchange the temperature of water and the matrix

are almost the same in the neighborhood of the axis and decreases. This observation is supported by our numerical experiments. Thus, the time evolution of temperature in the top point of axis is the main information in determination of transmission coefficient and, moreover, also heat conduction coefficient of the matrix.

To determine the boundary heat transmission coefficient we consider saturated sample with constant temperature field in porous media. The sample boundary is flow isolated (except of the top and bottom). The external temperature is constant and different from the initial temperature of the sample. We measure the time evolution temperature of the cumulated outflow water. The initial sample temperature and the temperature of infiltrated water from the top is the same. Water infiltrates from the cylindrical chambre with constant water level. In this scenario we have simple flow model and outflow boundary condition. This experimental scenario is used also in analysis of temperature isolation propertis of material applied on mantel surface in thin film form.

In our model setting we do not assume the temperature influence on the water flow, but it could be included. However, the heat transport and its mutual transmission with the porous matrix strongly depend on the water saturation in pores.

In the heat and mass transfer problem in facades we consider 2D problem which represents a cross-section of the facade, or cylindrical sample. The parallel vertical boundaries of the rectangle represent the building and outdoor environment contacts. In the case of cylindrical sample the left vertical boundary corresponds to its axis.

In the numerical method we use operator splitting method where we successively along small time interval separately solve water flow, then heat transport in water and then in matrix including heat exchange. In the solution of water flow we follow the approximation strategy introduced in [5] and also used in well known software Hydrus (see [3]). To control the correctness of our numerical results we have developed also an approximation scheme (see [8] used only for 1D) based on the reduction of the governing parabolic equations to a stiff system of ordinary differential equations. This approximation solves simultaneously whole system, but computational time is significantly larger. The main reason is that the system is stiff and too large when using necessary space discretization. Comparisons justify our method which is significantly quicker and therefore applicable in the solution of inverse problems in mathematical model scaling. Moreover, present method could be efficiently used also for solving 3D problems.

2. Mathematical model.

2.1. Water flow model. Water saturation $\theta \in (\theta_r, \theta_s)$ (θ_r is irreducible saturation and θ_s is porosity) we rescale to effective saturation

$$\theta_{ef}(h) = \frac{\theta(h) - \theta_r}{\theta_s - \theta_r}.$$

Here, h ([cm]) is head and the fundamental empirical relation between saturation θ and h in terms of van Genuchten/Mualem empirical model (capillary/pressure law) is

$$\theta(h) = \theta_r + \frac{\theta_s - \theta_r}{(1 + (\alpha h)^n)^m}, \ \theta_{ef}(h) = 1 \quad \text{for } h \geq 0, \tag{2.1}$$

where $\alpha < 0, n > 1$ and $m (m = 1 - 1/n)$ are soil parameters. Hydraulic permeability K is modeled by

$$K(h) = K_s k(\theta_{ef}), \ \ k(\theta_{ef}) = \theta_{ef}^{\frac{1}{2}}(1 - (1 - \theta_{ef}^{\frac{1}{m}})^m)^2, \tag{2.2}$$

where K_s is hydraulic permeability for fully saturated porous media. Water flux $\vec{q}$

$$\vec{q} = (q^x, q^y), \quad \vec{q}(h) = -K(h)(\nabla h - e_y),$$

where e_y is a unit vector in direction y representing gravitational driving force. Richards equation is of the form

$$\partial_t \theta(h) - div(K(h)(\nabla h - e_y)) = 0 \tag{2.3}$$

with the corresponding boundary conditions which will be specified in numerical experiments.

2.2. Heat energy in the water. Conservation of water heat energy is expressed in PDE

$$c_v \partial_t(\theta T_w) - div(-c_v \vec{q} T_w + (D_o \theta + \bar{D})\nabla T_w) = \sigma\theta(T_w - T_m) \tag{2.4}$$

where T_w is temperature of water, c_v is heat capacity of unite water volume, σ is transmission coefficient at the heat exchange with the matrix. Convective part is $c_v \vec{q} T_w$ and the diffusion/dispersion are characterized by molecular diffusion coefficient D_o and dispersion matrix $\bar{D}$, where

$$\bar{D} = \begin{pmatrix} D_{1,1} & D_{1,2} \\ D_{2,1} & D_{2,2} \end{pmatrix} = \begin{pmatrix} \alpha_L((q^x)^2 + \alpha_T((q^y)^2 & (\alpha_L - \alpha_T)(q^x q^y) \\ (\alpha_L - \alpha_T)(q^x q^y) & \alpha_L((q^y)^2 + \alpha_T((q^x)^2 \end{pmatrix} \frac{1}{|\vec{q}|}$$

Here, α_L, α_T are longitudinal and transversal dispersion coefficients. The corresponding initial and boundary conditions will be specified in the numnerical experiments.

2.3. Heat conduction in the matrix. We assume the simple heat conduction model in the matrix

$$c_m \partial_t T_m - \lambda \Delta T_m = \sigma\theta(T_w - T_m). \tag{2.5}$$

where T_m - matrix temperature, λ - heat conduction coefficient and c_m- heat capacity of the matrix.

For simplicity, we assume that on the boundary there are presribed fluxes or values of the unknown h, T_w, T_m and a combination of them.

2.4. Boundary conditions. Our solution domain Ω is a rectangle $(x, y) \in (0, X) \times (0, Y)$ and $t \in (0, \Upsilon)$. We consider the following boundary and initial conditions in our numerical solution drawn in Fig. 2.1

$$\begin{aligned} &\partial_y T_m = 0, \quad QT^y = 0, \quad h = h_0 && \text{on } (0, X) \times \{0\} \times (0, \Upsilon) \\ &\partial_y T_m = 0, \quad QT^y = 0, \quad q^y = 0 && \text{on } (0, X) \times \{Y\} \times (0, \Upsilon) \\ &T_m = 20, \quad T_w = 20, \quad h = -200 && \text{on } (0, X) \times (0, Y) \times \{0\}. \end{aligned}$$

The boundary conditions on $\{X\} \times (0, Y) \times (0, \Upsilon)$ are in the form

$$\partial_x T_m = \sigma_{m,r}(TM_r - T_m), \; QT^x = \sigma_{w,r}(TW_r - T_m), \; q^x = \sigma_{ww,r}(HW_r - h)$$

and on $\{0\} \times (0, Y) \times (0, \Upsilon)$

$$-\partial_x T_m = \sigma_{m,l}(TM_l - T_m), \; -QT^x = \sigma_{w,l}(TW_l - T_w), \; -q^x = \sigma_{ww,l}(HW_l - h),$$

where TM, TW, TH are external temperature and pressure sources, and $\sigma_{.,r}$, $\sigma_{.,l}$ are corresponding boundary transmission coefficients. The boundary flux conditions could be changed to Dirichlet boundary conditions.

2.5. Mathematical model in cylindrical coordinates. Consider the cylinder with radius R and height Y. Using cylindrical coordinates (r, y) in (2.3), (2.4) , (2.5) we obtain

$$\partial_t \theta(h) = \frac{1}{r}\partial_r(rK(h)\partial_r h) + \partial_y(K(h)(\partial_y h - 1)) \tag{2.6}$$

for water flow

$$c_v \partial_t(\theta T_w) - \left(\frac{1}{r}\partial_r(rQT^r) + \partial_y(QT^y)\right) = \sigma\theta(T_w - T_m) \tag{2.7}$$

for heat transport in water and

$$c_m \partial_t T_m - \lambda\left(\frac{1}{r}\partial_r(rQT_m^r) + \partial_y(\partial_y T_m)\right) = \sigma\theta(T_w - T_m).$$

for heat conduction in the matrix, where

$$\mathbf{q} = -(q^r, q^y)^T,\ q^r = K(h)\partial_r h,\ q^y = K(h)(\partial_z h - 1), \tag{2.8}$$

$$QT^r = -q^r T_w + \theta(D_{1,1}\partial_r T_w + D_{1,2}\partial_y T_w + D_o\theta, \tag{2.9}$$

$$QT^y = -q^y T_w + \theta(D_{2,1}\partial_r T_w + D_{2,2}\partial_y T_w + D_o\theta,\ QT_m^r = \partial_r T_m. \tag{2.10}$$

2.6. Model data and corresponding numerical solution for cylindrical sample. Our solution domain $R = X = 10, Y = 10$. In our numerical experiments we assume the following model data ([CGS] units) as "standard data" : $\theta_0 = 0.38$, $\theta_r = 0$, $K_s = 2.4\ 10^{-4}$, $\alpha = 0.0189$, $n = 2.81$, $D_o = 0.03$, $\lambda = 0.3$, $\alpha_L = 1$, $\alpha_T = \frac{1}{10}$, $c_v = c_m = 1$ and $\sigma = 1$. These data correspond to a limestone.
We consider the boundaries $(0, 10) \times 0$ and $(0, 10) \times 10$ with zero heat and flow fluxes (isolation). On the boundary $10 \times (0, 10)$ the hydrostatic pressure $h = (Y - y), y \in (0, Y)$ is prescribed and $T_w = 0$. On the axis $10 \times (0, 10)$ we have $q^r = 0,\ QT^r = 0$. We consider heat isolation for matrix boundaries.
The initial conditions are $h = -200$ and $T_w = T_m = 20$. In the Fig. 2.1 we draw the corresponding flow and temperature fields for the cylinder cross-section at the time moment $t = 60s$.

3. Numerical method. In our approximation scheme we apply a flexible time stepping and a finite volume method in space variables. We consider uniform partition of the domain with $(N_x, N_y) = (31, 31)$ grid points $(x_i, y_j) = (i\Delta x, j\Delta y),\ i, j = 0, 1, ..., 30,\ \Delta x = \frac{X}{N_x - 1}, \Delta y = \frac{Y}{N_y - 1}$. The time derivative we approximate by backwards difference and then we integrate our system over the angular control volume $V_{i,j}$ with the corners $x_{i\pm\frac{1}{2}}, y_{j\pm\frac{1}{2}}$ and with the length $(\Delta x, \Delta y)$ of the edges. Then, our approximation linked with the inner grid point (x_i, y_j) at the time $t = t_k$ is

$$\Delta x\Delta y\frac{\theta(h) - \theta(h^{k-1})}{\tau} - \Delta y\left[\frac{K(h_{i+1}) + K(h)}{2}\left(\frac{h_{i+1} - h}{\Delta x}\right)\right]$$
$$+\Delta y\left[\frac{K(h) + K(h_{i-1})}{2}\left(\frac{h - h_{i-1}}{\Delta x}\right)\right] - \Delta x\left[\frac{K(h_{j+1}) + K(h)}{2}\left(\frac{h_{j+1} - h}{\Delta y} - 1\right)\right]$$
$$+\Delta x\left[\frac{K(h) + K(h_{j-1})}{2}\left(\frac{h - h_{j-1}}{\Delta y} - 1\right)\right] = 0.$$

Omitted indices are of values $\{i, j, k\}$.

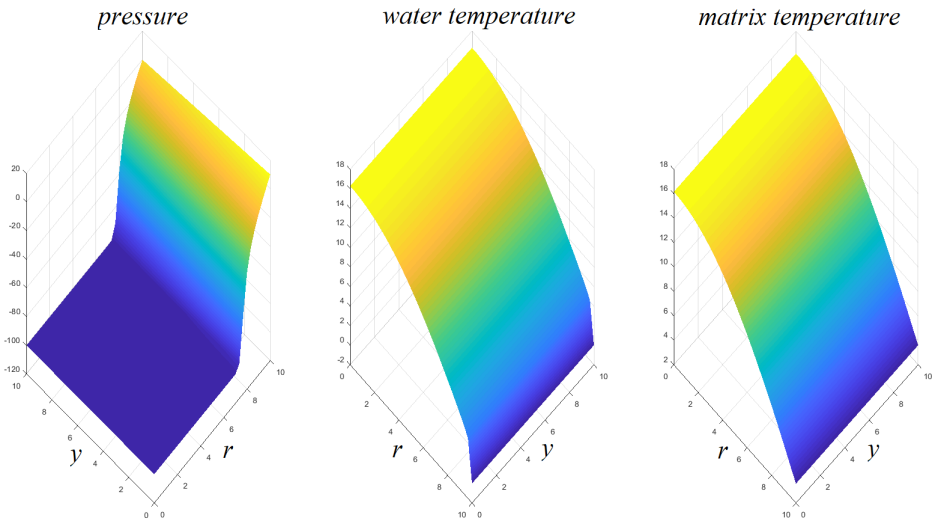

FIG. 2.1. *Water pressure h and temperatures T_w, T_m in cylinder at $t = 60s$*

3.1. Quasi-Newton linearization. In each (x_i, y_j) we linearize θ in terms of h iteratively (with iteration parameter l) following [Cellia at all][5] in the following way

$$\frac{\theta(h^{k,l+1}) - \theta(h^{k-1})}{\tau} = C^{k,l}\frac{h^{k,l+1} - h^{k,l}}{\tau} + \frac{\theta^{k,l} - \theta^{k-1}}{\tau} \tag{3.1}$$

where

$$C^{k,l} = \frac{\partial\theta^{k,l}}{\partial h^{k,l}} = (\theta_s - \theta_r)(1-n)\alpha(\alpha h^{k,l})^{n-1}(1 + (\alpha h^{k,l})^n)^{-(m+1)}$$

for $h^{k,l} < 0$, else $C^{k,l} = 0$. We stop iterations for $l = l^*$, when

$$|h^{k,l^*} - h^{k,l^*-1}| \leq Tollerance, \text{ then we put } h^k := h^{k,l^*}.$$

Finally. we replace the nonlinear term $K(h^k)$ by $K(h^{k,l})$. Our approximation scheme then becomes linear in terms of $h^{k,l+1}$. Generally, we speed up the iteration by a special construction of starting point $h^{k,0} \approx h^{k-1}$ and eventually using suitable damping parameter in solving corresponding linearized system.
The complex system is solved by **operator splitting method**. To obtain an approximate solution for temperatures in water and matrix at the time section $t = t_k$, starting from $t = t_{k-1}$ we use flow characteristics obtained at $t = t_k$ for $\theta^k, h^k, \vec{q}^k$, and D^k.

3.2. Approximation scheme for water temperature. For $T_w(\equiv T), T_m$ at (x_i, y_j) for $t = t_k$ we obtain by finite volume

$$
\begin{aligned}
&c_v\theta\frac{T-T^{k-1}}{\tau}\Delta x\Delta y\\
&-\Delta y\left[-c_v q^x_{i+\frac12}\frac{T_{i+1}+T_i}{2}+D_{1,1,i+\frac12}\frac{T_{i+1}-T_i}{\Delta x}+D_{1,2,i+\frac12}\frac{T_{i+1,j+1}+T_{i,j+1}-T_{i+1,j-1}-T_{i,j-1}}{4\Delta y}\right]\\
&+\Delta y\left[-c_v q^x_{i-\frac12}\frac{T_i+T_{i-1}}{2}+D_{1,1,i-\frac12}\frac{T_i-T_{i-1}}{\Delta x}+D_{1,2,i-\frac12}\frac{T_{i,j+1}+T_{i-1,j+1}-T_{i,j-1}-T_{i-1,j-1}}{4\Delta y}\right]\\
&-\Delta x\left[-c_v q^y_{j+\frac12}\frac{T_{j+1}+T_j}{2}+D_{2,2,j+\frac12}\frac{T_{j+1}-T_j}{\Delta y}+D_{2,1,j+\frac12}\frac{T_{i+1,j+1}+T_{i+1,j}-T_{i-1,j+1}-T_{i-1,j}}{4\Delta x}\right]\\
&+\Delta x\left[-c_v q^y_{j-\frac12}\frac{T_j+T_{j-1}}{2}+D_{2,2,j-\frac12}\frac{T_j-T_{j-1}}{\Delta y}+D_{2,1,j-\frac12}\frac{T_{i+1,j}+T_{i+1,j-1}-T_{i-1,j}-T_{i-1,j-1}}{4\Delta x}\right]\\
&=\Delta x\Delta y\sigma\theta^k(T_m-T_w).
\end{aligned}
\tag{3.2}
$$

3.3. Approximation of $\vec{q}$ and D in middle points. We approximate $\vec{q}$ and D in middle points by

$$
q^x_{i\pm\frac12}=-\frac{K(h_{i\pm1})+K(h_i)}{2}\left(\frac{\pm h_{i\pm1}\mp h_i}{\Delta x}\right),\ q^y_{j\pm\frac12}=-\frac{K(h_{j\pm1})+K(h_j)}{2}\left(\frac{\pm h_{j\pm1}\mp h_j}{\Delta y}-1\right)
$$

$$
\begin{aligned}
q^y_{i\pm\frac12}&=-\frac{K(h_{i\pm1})+K(h_i)}{2}\left(\frac{h_{i\pm1,j+1}+h_{i,j+1}-h_{i\pm1,j-1}-h_{i,j-1}}{4\Delta y}-1\right)\\
q^x_{j\pm\frac12}&=-\frac{K(h_{j\pm1})+K(h_i)}{2}\left(\frac{h_{i+1,j\pm1}+h_{i+1,j}-h_{i-1,j\pm1}-h_{i-1,j}}{4\Delta x}\right),\\
D_{1,1,i\pm\frac12}&=\left(\alpha_L(q^x_{i\pm\frac12})^2+\alpha_T(q^y_{i\pm\frac12})^2\right)\frac{1}{\sqrt{(q^x_{i\pm\frac12})^2+(q^y_{i\pm\frac12})^2}}+\lambda_t\theta_{i\pm\frac12}\\
D_{1,2,i\pm\frac12}&=(\alpha_L-\alpha_T)q^x_{i\pm\frac12}q^y_{i\pm\frac12}\frac{1}{\sqrt{(q^x_{i\pm\frac12})^2+(q^y_{i\pm\frac12})^2}}
\end{aligned}
$$

and analogously

$$
D_{2,2,j\pm\frac12}=D_{1,1,i\pm\frac12}\ (i\leftrightarrow j;\alpha_L\leftrightarrow\alpha_T);\ D_{2,1,j\pm\frac12}=D_{1,2,i\pm\frac12}\ (i\leftrightarrow j).
$$

3.4. Approximation scheme for matrix temperature. The governing PDE with BC and IC

$$
c_m\partial_t T_m-\lambda\Delta T_m=\sigma\theta(T_w-T_m)\tag{3.3}
$$

$T_m = T^k_m$ is approximated by FVM ((x_i, y_j), $t = t_k$) to

$$
\begin{aligned}
&c_m\frac{T_m-T^{k-1}_m}{\tau}\Delta x\Delta y-\Delta y\lambda\left[\frac{T_{m\ i+1}-T_{m\ i}}{\Delta x}-\frac{T_{m\ i}-T_{m\ i-1}}{\Delta x}\right]\\
&-\Delta x\lambda\left[\frac{T_{m\ j+1}-T_{m\ j}}{\Delta y}-\frac{T_{m\ j}-T_{m\ j-1}}{\Delta y}\right]=\Delta x\Delta y\sigma\theta^k(T_m-T_w).
\end{aligned}
\tag{3.4}
$$

3.5. Solution of the inverse problem to determine σ, λ. Measuring the temperature of water and matrix in the sample is a difficult task. So we propose the infiltration scenario which enables us to measure σ. There is uniformly distributed small amount of water $h = -100$ in the sample and the initial temperature of water and matrix are the same $T_w = T_m = 20C$. The top and bottom of the sample are isolated (zero water and temperature fluxes). The top boundary is free and from the bottom we let water to infiltrate. Water infiltrates by hydraulic pressure from the mantel. The temperature of infiltrating water is $0C$ We are measuring the water temperature on the top boundary. The model data are the same as data in Fig. 2.1. The time evolution of the computed temperature on the top is presented in the Fig. 3.1 (blue line).

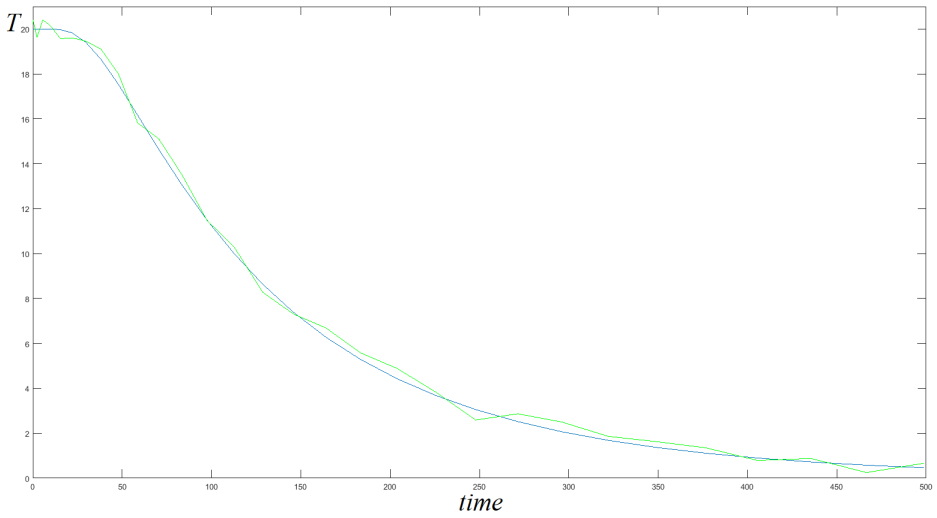

FIG. 3.1. *Time evolution of temperature in top of the axis*

The computed data have been perturbed by the $0.5C$ of noise using the random function (green line). These were considered to be measured data. Then, we forgot our transmission coefficient σ $(= 1)$, and matrix heat conduction coefficient λ $(= 0.3)$ and we used an iteration procedure to minimize the discrepancy between the measured data and the computed data.
The optimal point σ_{opt}, λ_{opt} (with respect to the given tolerance) is taken for the required transmission and conduction coefficients. We verify its stability with respect to the choice of starting points in iteration procedure. All measured data correspond to different random noises. During the measured time interval $t \in (0, 500)$ we have used only 31 time moments.

The obtained results with different starting points are collected in Table 3.1. Used starting points are combinations of $\sigma \in \{0.5, 1.5\}$ and $\lambda \in \{0.1, 0.5\}$. The final value does not depend on the starting point. However, it can be noticed that values of parameters σ, λ slightly mutually interfer. There is always one that is lower than the exact value while the other is changed in a opposite way.

3.6. Solution of the inverse problem to determine $\sigma_{m,r}$, $\sigma_{w,r}$. In the fact, we shall assume that $\sigma_{m,r} = \sigma_{w,r} := \sigma_B$ and in this case we obtain the stable results. When they differ, the determination procedure is unstable and one can note the substitution effects between them. In the determination procedure we proceed as in the

TABLE 3.1
Optimal values of λ, σ

start	σ, λ	σ, λ
$[0.5, 0.1]$	$[1.0475, 0.2974]$	$[0.9842, 0.3082]$
$[1.5, 0.1]$	$[0.9547, 0.3277]$	$[1.0212, 0.2945]$
$[0.5, 0.5]$	$[1.0324, 0.2821]$	$[0.9771, 0.3114]$
$[1.5, 0.5]$	$[0.9685, 0.2854]$	$[1.0389, 0.2901]$

previous section determining (σ, λ). In our experiment we use the "standard" model data with the following changes. The sample is fully saturated and the temperature of the sample is $20C$. The mantel of the cylinder is water flow isolated. The temperature outside the cylinder matle is $15C$. The temperature field in the sample is drawn in the Fig. 3.2 at the time moment $t = 1500s$. Water is infiltrated into sample throught the smaller circle on top ($R_{in} = 5$) with pressure 5 and temperature 20. Water flows out from the sample bottom. Temperature time evolution of the cumulated outflow water is drawn in Fig. 3.3.

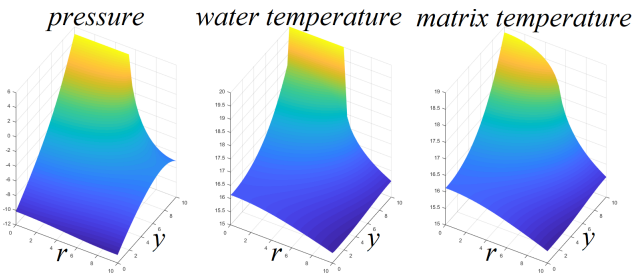

FIG. 3.2. *Pressure and temperatures at* $t = 1500$

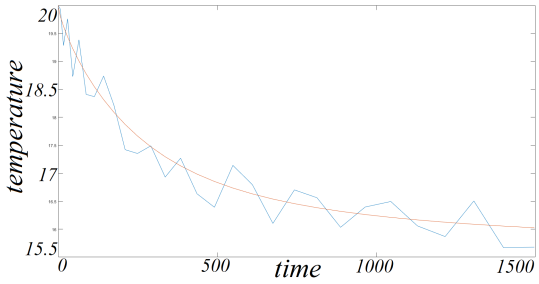

FIG. 3.3. *Temperature of cumulated outflow water*

To determine σ_B $(= 1)$ we are using measurements from the blue line in Fig. 3.3 which correspond to $0.5C$ of noise using the random function. As a starting point for σ_B we use $\{0.5, 11.5\}$ with two different noise applications. The obtained optimal values are collected in Table 3.2. We present there also experiments corresponding to 0.1 noise.

Originally, we have solved our system using its approximation by a corresponding stiff system of ODE, where space discretizarion is realized by finite volume method. In this case we do not use operator splitting method. The solution coincides with that one obtained by present method up to the first two digits when ruther dense grid points are used. But the present method is signifficantly faster and more suitable in

TABLE 3.2
Optimal values of α_L

start	σ_B (0.5)	σ_B (0.5) —	σ_B (0.1)	σ_B (0.1)
0.5	0.90322	1.13708	1.03359	0.98857
1.5	1.18073	1.11269	0.96027	1.01879

solving inverse problems. In 1D we have compared solutions with that ones in [8], [3] and [4].

4. Summary.

- Numerical modeling of heat exchange arising in water infiltration in unsaturated porous media is discussed.
- Efficient numerical method is developed on the base of time stepping, operator splitting and FVM.
- An infiltration scenario is proposed to determine the heat transmission coefficient inside the porous media by solution of inverse problem.
- Also a scenario is proposed to determine the boundary heat transmission coefficient.
- The efficiency of the numerical method is demonstrated by numerical experiments.

REFERENCES

[1] J. BEAR, A. H.-D. CHENG, *Modeling Groundwater Flow and Contaminant Transport*, Springer 2010, V.23 .

[2] D. CONSTALES, J. KAČUR, *Determination of soil parameters via the solution of inverse problems in infiltration*, Computational Geosciences 5 (2004), pp. 25–46.

[3] J. ŠIMUNEK, M. ŠEJNA, H. SAITO, M. SAKAI, M. TH. VAN GENUCHTEN, *The Hydrus-1D Software Package for Simulating the Movement of Water*, Heat, and Multiple Solutes in Variably Saturated Media, (2013).

[4] J. ŠIMUNEK, J. R. NIMO, *Estimating soil hydraulic parameters from transient flow experiments in a centrifuge using parameter optimization technique*, Water Resour. Res. 41, W04015 (2005).

[5] M. A. CELIA, Z. BOULOUTAS, *A general mass-conservative numerical solution for the unsaturated flow equation*, Water Resour. Res. 26 (1990), pp. 1483–1496.

[6] J. KAČUR, P. MIHALA, M. TÓTH, *Determination of soil parameters under gravitation and centrifugal forces in 3D infiltration*, Vseas transactions on heat and mass tranfer, Vol. 11, (2016), pp. 115–120.

[7] D. CONSTALES, J. KAČUR, B. MALENGIER, *A precise numerical scheme for contaminant transport in dual-well flow*, Water Resources Research, vol. 39(10), (2003), pp. 1292–1303,

[8] J. KAČUR , J. MINÁR, *A benchmark solution for infiltration and adsorption of polluted water into unsaturated-saturated porous media*, Transport in porous media, vol. 97, (2013), pp. 223–239.

[9] T. L. BERGMAN, A. S. LAVINE, F. P. INCROPERA, D. P. DEWITT, *Fundamentals of heat and mass transfer*, John Wiley and Sons, 7th edition, (2011), ISBN 13 978-0470-50197-9.